Fabrication of an inexpensive injection molding instrument for rapid prototyping of high precision parts

David M. Wirth, Leonard G. McCline, Jonathan K. Pokorski

PII: S0032-3861(22)01009-6

DOI: https://doi.org/10.1016/j.polymer.2022.125521

Reference: JPOL 125521

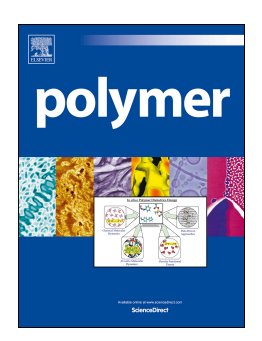
To appear in: Polymer

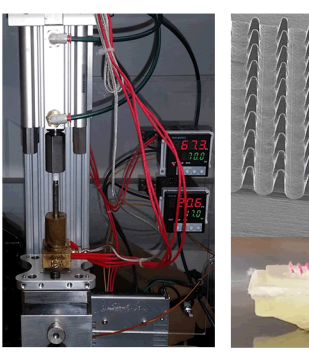
Received Date: 22 August 2022
Revised Date: 8 November 2022
Accepted Date: 13 November 2022

Please cite this article as: Wirth DM, McCline LG, Pokorski JK, Fabrication of an inexpensive injection molding instrument for rapid prototyping of high precision parts, *Polymer* (2022), doi: https://doi.org/10.1016/j.polymer.2022.125521.

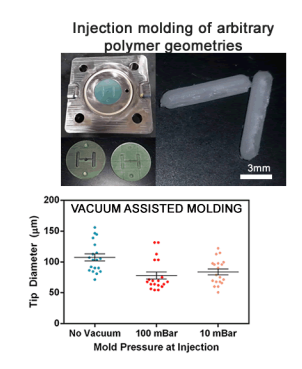
This is a PDF file of an article that has undergone enhancements after acceptance, such as the addition of a cover page and metadata, and formatting for readability, but it is not yet the definitive version of record. This version will undergo additional copyediting, typesetting and review before it is published in its final form, but we are providing this version to give early visibility of the article. Please note that, during the production process, errors may be discovered which could affect the content, and all legal disclaimers that apply to the journal pertain.

© 2022 Published by Elsevier Ltd.









John Alexandra de la companya della companya della companya de la companya della companya della

Fabrication of an Inexpensive Injection Molding Instrument for Rapid

Prototyping of High Precision Parts

David M. Wirth, Leonard G. McCline, and Jonathan K. Pokorski*

Department of NanoEngineering, University of California, Jacobs School of Engineering, La

Jolla, California 92093, United States

*Corresponding Author

Email Address: jpokorski@ucsd.edu

Phone Number: 858-246-3183

Address: 9500 Gilman Dr., SME Building 243J, La Jolla, California 92093, United States

Abstract:

Polymeric drug delivery devices are among the most promising avenues to improve

equitable distribution of life saving medications throughout the world. At present, most research

into manufacturing of these devices relies heavily on solvent-based methods, limiting scalability,

reproducible manufacture, and leading to potentially cytotoxicity. Solvent-free polymeric

biomedical implants manufactured through traditional thermal processing methods eliminate the

bulk of these concerns, however they are difficult to manufacture in a research laboratory setting.

Investigation of techniques, such as injection molding, have been limited in the past due to the

high upfront cost of polymer equipment and the large scale necessary to conduct pilot

experiments. This study describes a low cost bench-top milliliter-volume vacuum injection-

molding system, capable of pilot-scale injection molding of small shapes of arbitrary geometry.

The plans presented herein open this convenient and scalable manufacturing technique to

academic research laboratories interested in pilot-scale experiments with polymeric devices specifically aimed at polymers relevant for polymeric drug or vaccine delivery. Demonstration of the fabrication of simple geometric parts and solvent-free polymeric microneedle patches is described. In particular, microneedle patches demonstrate the capabilities and limitations to produce fine feature sizes for biomedically relevant products.

Keywords: Melt processing | injection molding | vaccine distribution | drug delivery | scalable manufacturing | polymer engineering | microneedles | controlled release

Introduction:

Research into the injection molding (IM) of high value polymeric materials is a promising avenue which has been historically limited due to the high cost of traditional IM equipment. Barriers to the field are created by the difficulty of constructing a high pressure, high temperature durable mechanical apparatus, liquid cooling, hydraulic systems and/or mechanical augurs. [1,2] Historically, IM as a technique was first developed in the late 1800's and matured quickly after the discovery of Bakelite [3] in the early 1900's. IM is carried out by forcing molten polymer through an orifice into a mold cavity where it expands and solidifies. An augur, metering screw or piston is used to exert driving force on the polymer to move it through the barrel where it melts, and once liquefied is forced through the nozzle and into the mold consisting of a desired shape. [4] The augur or piston then retracts and spring loaded ejector pins assist in removing the solid part from the mold, clearing the cavity for the next injection. This cycle is very simple and may be highly automated, allowing industrial users to manufacture large volumes of identical parts automatically with little supervision. Industrial injection mold

pressures are normally between 70-112 MPa.^[5] Small scale systems intended for testing, analysis and demonstration may be as low as 10-60 MPa.^[6] The power of IM lends itself well to industrial manufacturing in order to mass-produce parts continuously at very high production rates.^[7] The rapid solidification of polymer in the mold is usually assisted by water cooling channels drilled throughout the mold block, but such water cooling is mainly required to achieve fast cycle times and is not essential for the operation of a small scale pilot IM system.

In recent years, a number of microinjection molding systems have sought to offer simpler, cheaper and/or smaller scale alternatives to a mass production IM system for bench-top or laboratory scale applications, allowing for R&D and pilot scale studies to take place with injection volumes as low as 1 cm³, with some specialty systems offering volumes as low as 82 mm³.^[8] However, such systems are generally high in cost and difficult to adapt to research settings, making IM a seldom-explored technique in academic biomaterial research despite its high scalability and unique advantages over other techniques.^[9]

In our recent work^[10] we demonstrated a polymer melt processing system which was cost-reduced and scaled down to fill this capability gap with the hope of expanding research into IM as a manufacturing technique for high-value materials such as therapeutic drugs and nanomaterials.^[11,12] However, despite our success at cost-reduction and decreasing the dead volume to ensure minimal waste, its maximum capacity was limited by the size of a commercial 3D printer hot-end. In this manuscript our design has been iterated to include custom metal parts to increase the melt volume and produce larger part geometries. The newly designed instrumentation affords far greater flexibility to design a modular system which can create custom and arbitrary geometries as well as solvent-free microneedle patches and biomaterial implants.

Polymer drug delivery devices are an active area of research and have been used to treat various diseases and infections.^[13–18] Despite inherent difficulties in scaling and storage, these devices are ordinarily fabricated with solvent-based centrifugal or drop-casting due to the flexible material requirements and low waste of these processing methods. However, residual solvent in such devices may limit their shelf life. Similar to solvent casting, IM is commonly used to produce objects with various shapes and functions.^[4,19,20] Unlike solvent casting, IM production can be extremely rapid and devices produced via IM do not need excessive drying to remove potentially trapped solvents. Despite the advantages of IM over traditional solvent casting, IM as a manufacturing technique is typically overlooked by many laboratories due to the high budget and/or feedstock production capabilities required for its use.^[21]

The melt-processing of polymers is commonly used in cosmetic and pharmaceutical packaging, but more recently has been the subject of research for the production of biomedical devices including controlled release drug delivery methods including biopolymer implants and microneedle patches. [22–26] Melt processing techniques can allow researchers to tailor the shape, dimensions, or release properties of implantable devices within the body to deliver drugs where and when they are needed for maximum therapeutic effect. [27–29] Furthermore, the IM process applies both heat and high pressure to the formed polymer, sterilizing the molded components, reducing microbial contamination, and potentially improving the bioavailability of poorly soluble drugs administered via this method. [30–32] Recently, the need for versatile and highly scalable drug delivery platforms has been highlighted by the COVID-19 pandemic. [33] Nearly 20 million children were under-vaccinated or un-vaccinated in 2019 and 2.8 million vaccines were lost in five countries due to cold chain failures, with less than 10% of countries meeting WHO recommendations for effective vaccine management practices [34,35]. The rapid manufacturing and

worldwide distribution of delivery devices made possible by IM production could provide substantial advantages in terms of addressing future pandemics in terms of easing the burden on HCP, and reducing the need for cold-chain storage of vaccines.^[10,11,29,36,37] A single-dose slow-release implant or microneedle patch based vaccine fabricated using high-throughput IM techniques could accelerate production, distribution and reduce reliance on the cold chain.

In this work we have designed an instrument which can IM many polymers into arbitrary geometries. We chose microneedles as a test-bed for the system due to their fine feature size and high aspect ratio, thus allowing us to quantify the performance of our high-resolution vacuum-assisted injection molding system and assess the potential utility of IM-produced biopolymer devices.

Methods:

Materials, chemicals, sources, equipment and software are described in the supplemental information.

Construction of Pilot-Scale Injection Molding System:

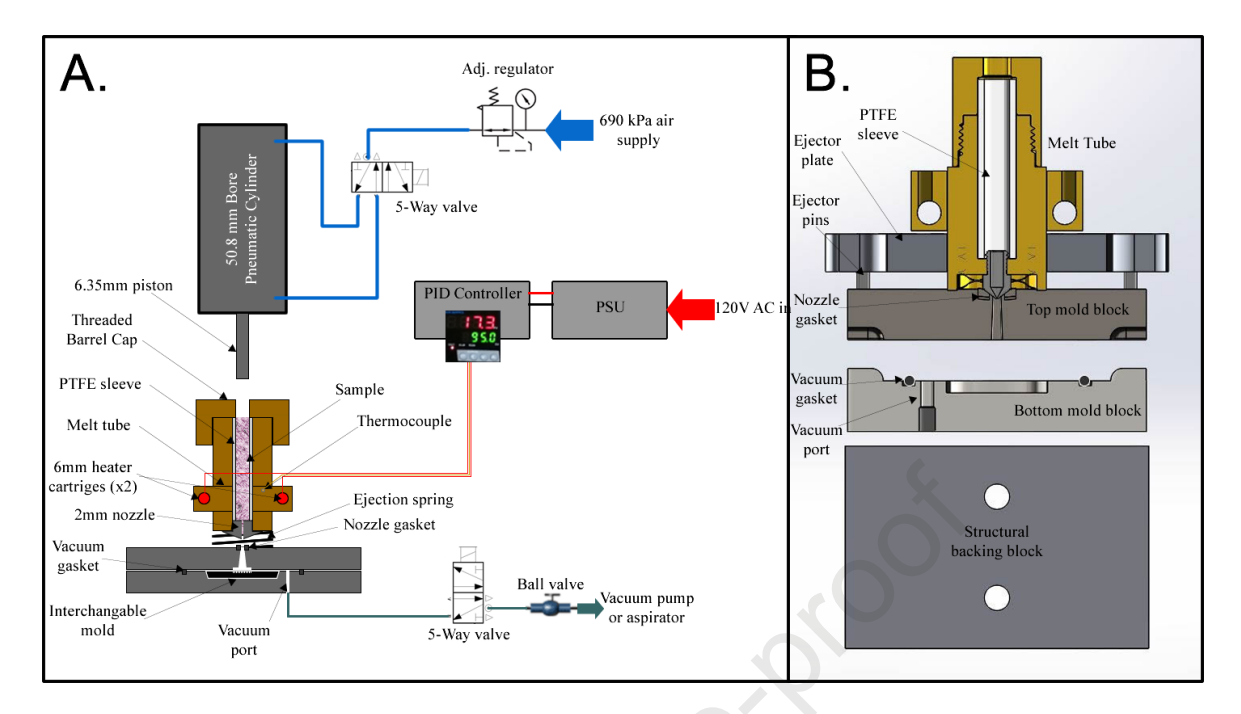


Figure 1: Injection molding system design - A) Schematic representation of injection molding system, B) computer aided drafting cross sectional model of critical design elements in the injection molding system

The design of the Pilot-Scale Injection Molding System (**Figure 1**) iterated upon the design of the Desktop Injection Molding System in our earlier work and is briefly described below. [10] The supporting information gives exact specification (**Table S1**, **Figures S1-S5**), as well as CAD files, to reconstruct the device. The system was constructed around a 0.25" (6.35 mm) diameter piston. Due to lab air pressure of 690 kPa, we used a 2" (50.8 mm) bore actuator to exert the necessary force on our larger diameter piston. The larger 2" bore actuator was permanently bolted onto a 3x1" T-slotted aluminum frame where the mold block also slides using a handle to manually increase the friction between the mold block assembly and the rails. Clamping force from the handle creates friction between the backing block and 3" T-slot, which alone was sufficient to hold the mold block in place even at maximum actuator pressure. Two ceramic cartridge heaters and a thermocouple were connected to a commercial PID controller, which was powered by a 300 W 12 V power supply.

Polymer Blend Fabrication:

Several polymer samples (Table 1) were successfully prepared for injection molding.

Table 1: Composition of samples prepared for injection molding.

#	Polymer(s)	Ratio	Polymer T _m	Polymer T _g	Injection	Injection
		(wt%:wt%)	(°C)	(°C)	Temp.	Pressure
					(°C)	(MPa)
1	PCL	N/A	$60^{[38]}$	-60 ^[38]	55-90	9-50
2	PEG 100kDa	N/A	65 ^[39]	-40 ^[39]	60-100	35-42
3	PEG 100kDa/ PVP K15	90:10	~65	<-35	80-100	35-42
4	PEG 100kDa/ 8kDa/ PVP K15	80:10:10	~65	<-35	80-100	35-42
5	PLGA [†]	N/A	N/A	~42.6 ^[40]	80-120	35-42

[†]PLGA is an amorphous polymer and exhibits no clear T_m

Pure polymers were obtained from commercial vendors (Chemicals and Sources are detailed in the Supplemental Information). The blends were fabricated by mixing the bulk powders at their respective ratios and placing them in an aluminum foil pouch on a hydraulic press heated to 100 °C. The mixture was heated, pressed, and then folded on itself three or more times to ensure proper homogenization. Characterization of the melting point of polymer blends along with the as-purchased Poly(lactic co-glycolic acid), (PLGA) was conducted via DSC (Figure S6).

Injection Mold Insert Fabrication:

A stainless steel mold holder (**Table S2** "M3/Bottom Mold") was CNC machined, into which an approx. 1" diameter mold "mold insert" can be placed. A variety of 3D printed insert molds for notional geometries were fashioned without the need to re-machine expensive metal components. The method to create such mold inserts in a laboratory setting is summarized in **Figure 2**. Because of the reinforcement provided by the steel mold holder, these mold inserts can be made from inexpensive polymeric materials which are easily replaceable. One sample layout for printable inserts is provided for a cylindrical implant shape (**Figure 2C/2F/2G**). Two other insert molds, a "smiley" face demonstration and spherical implants are shown in **Figure 2H/2I**.

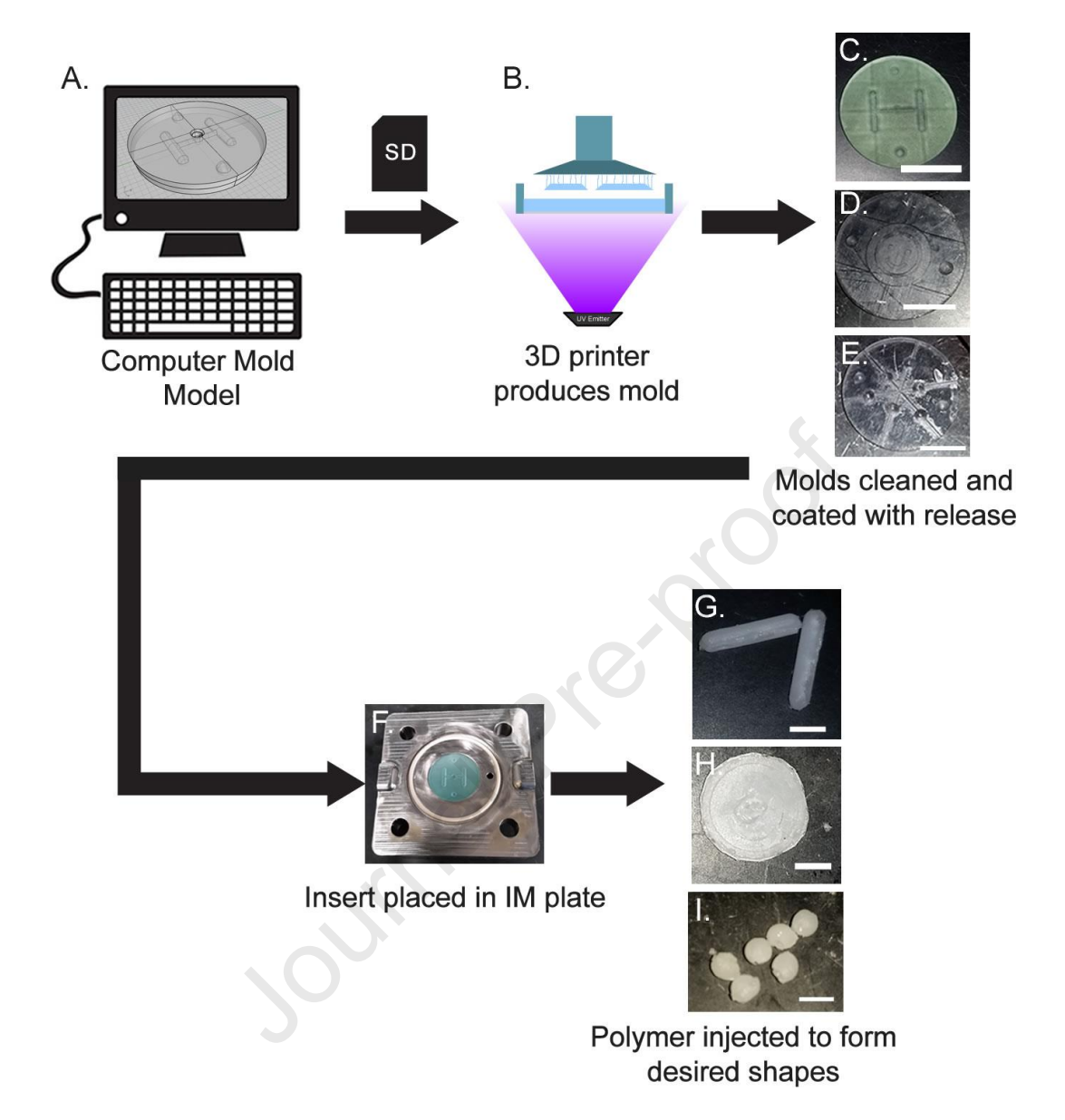


Figure 2: Procedure for forming insert injection molds for implants, scaffolds and other arbitrary shapes with millimeter-scale features. A) Mold is drawn on CAD and exported to as STL, B) resin 3D printer produces insert molds, C/D/E) molds are removed from printer, cleaned and coated with silicone mold release, F) placed in the machined IM plate, then G/H/I) injected with molten polymer and the resultant structures demolded. Scale bars: C,D,E: 10 mm, G,H,I: 3 mm.

The fabrication of these 3D printed insert molds was accomplished by first drafting the geometry to be fabricated on a suitable CAD program, and using a boolean subtraction tool to remove the desired geometry from two sides of a mold insert blank (IM_Insert_blank.stp). This was then exported as an STL and sliced using a suitable SLA/MSLA/DLP slicing utility (such as

Photon Workshop). The mold was then printed in resin (Siraya Blu or Siraya Fast Black), cleaned, washed and sprayed with mold release (CRC Silicone Mold Release #03302), placed in the Pilot-Scale IM System and injected with polymer. Fabrication of insert molds for arbitrary geometries may be 3D printed from ordinary SLA/DLP print resin using manufacturer specifications for layer exposure time and print parameters. In designing the 3D printed molds, it is important to reduce dead volume between the injection port and the vacuum ring by extending the upper mold insert into the cavity of the upper steel mold tool. Vent ports can be added to one or both sides of the insert to facilitate evacuation of the excess polymer after the mold insert cavity has been filled.

Fabrication of Microneedle Insert Molds:

A commercial PDMS negative microneedle mold was used as a template to a HEMA positive mold. First, a photocurable HEMA resin was added to the PDMS negative mold, then used as a transfer material to cast an insert from high temperature epoxy without sacrificing geometric details or concave needle sharpness. A detailed description of the fabrication instructions for the formation of microneedle array mold inserts, and print parameters for insert molds are detailed in the supplemental (**Figure S7-S15**), STL files and CAD diagrams for which can also be found in supplemental information. A simplified procedure for this transfer casting is shown in **Figure 3**.

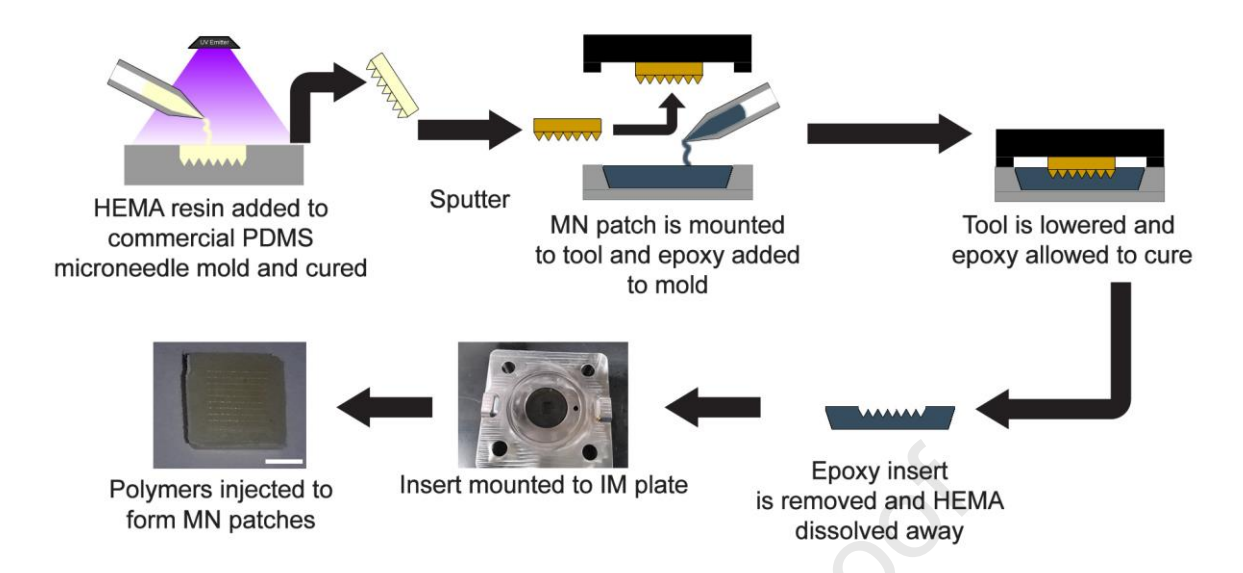


Figure 3: Diagram describing the procedure for fabricating IM microneedle patches. Scale bar: 3mm.

Injection Molding Procedure:

Injection molding was carried out by first coating all mold surfaces with silicone mold release, placing the mold insert in the steel bottom mold, then assembling the stack and connecting the vacuum line. Finely pulverized polymer (20 mesh or smaller) was then loaded into the melt tube. The melt tube was then heated electrically to the desired temperature and left to equilibrate for 2 minutes once the temperature was reached. The vacuum was then turned on and the setup was inspected to ensure the vacuum seal was good (no hissing noise). The desired injection pressure was dialed in on the regulator (see **Table 1** for injection pressures and temperatures), and the injection was carried out using the lever-actuated 5-way valve. After injection was complete, the pressure regulator was dialed to 0, and the line pressure allowed to vent. Then the vacuum was broken using the button valve on the vacuum line, and the heating was stopped. The vacuum line was disconnected and the top and bottom mold halves were left to cool for 5-10 minutes. The melt tube was also removed from the piston while the polymer was

molten and left to cool separately. After the mold halves cooled, the injection molded structures could be extracted and flashing removed with a pair of scissors or flush cutters (**Figure 4**). The setup could then be re-assembled and the process repeated for additional samples. The apparatus designed herein is capable of injection molding many other thermoplastic polymers. Best results are obtained with polymers with T_m below 120 °C, injected at 35-42 MPa.

Results and Discussion:

Pilot-Scale Injection Molding System Design:

The newly devised system was constructed to be capable of injecting up to 1.5 cm³ of polymer per injection, since a larger volume of polymer would likely be required for most applications of drug delivery devices. We intended our system to serve as a pilot-scale device which could be easily replicated and modified by others in the field. The system was constructed to investigate the feasibility of fabricating parts of arbitrary geometry via IM- for which we would need to test many different polymers and blend/composite formulations before arriving at one which was suitable. In keeping with these goals: we designed the system to accommodate ease of disassembly, and the barrel to ensure ease of cleaning so that various polymers and mold designs could be tested with minimal work. It was chiefly for this reason we chose to construct our pilot-scale system with a piston-based constant-pressure design rather than a more conventional augur-based constant-volume design. Such a design also allows for easy cleaning of all components and minimal dead volume for rapid prototyping of molds and materials.

Due to the larger barrel diameter of our new system, a larger piston was needed, and in order to maintain similar injection pressure on the molten plastic (~50 MPa) with the larger piston, a larger pneumatic actuator or a higher pressure would consequently be required. We

opted to use a larger actuator because it would eliminate the need for a costly high pressure pump. Furthermore, keeping the pressure low would increase overall system safety, and allow for others to reproduce our system as 690 kPa is a common supply pressure for in-house compressed air.

The system was originally designed for the mold block to slide along 9/16" shafts but such reinforcement was found to be unnecessary and friction between the backing block and 3" T-slot alone was sufficient to hold the mold block in place even at maximum actuator pressure.

Two ceramic cartridge heaters and a thermocouple were used for heating of the barrel, however after testing this setup, it is recommended to use the highest wattage 6 mm cartridge heaters available - using standard 30 W cartridge heaters will result in excessively long warm-up times and may require external insulation of the melt tube.

Discussion of the Fabrication of 3D Printed Insert Molds:

3D printed insert molds are easily designed and adapted to any desired geometry. It was important to design insert molds from a rigid, heat resistant 3D print resin. However, because the resin insert is only briefly exposed to elevated temperatures, we suspect that many commercial SLA or DLP resins would work in this application, albeit with limited durability. We used primarily Siraya Tech resins for their high toughness, Siraya Blu was particularly robust and we employed it for the majority of our parts. Siraya Fast Smokey Black was also found to be suitable for 3D printed insert molds. These 3D printed inserts lasted dozens of injection runs with minimal degradation.

Fabrication of Microneedle Insert Molds:

pHEMA was chosen as the material of choice for the transfer of geometry from the PDMS negative mold to the epoxy insert because it could be cured in a reasonable timeframe without the use of additional crosslinkers, using an ordinary photoinitiator, while still forming a rigid resultant polymer which could retain its shape and small geometric features after demolding from the silicone. It could then be dissolved in solvents such as DMSO/HNO₃ to remove all traces from the fine features of the resultant mold.

We found that microneedle transfer blanks could also be produced from PVP rather than pHEMA, and the DMSO/HNO3 washings replaced with warm water. While this greatly simplified the procedure and eliminates the need for a tricky and potentially dangerous aqua regia sonication step, it introduced defects in the mold which are discussed and characterized in greater detail in the supplemental information.

It is important to note that in a mass production environment, where cost is not an obstacle, such a mold insert could be made using electrochemical machining techniques from microporous stainless steel and the pre-vacuum applied through the bulk of the microporous insert to allow for even higher fidelity, repeatability and tip sharpness of the microneedles. Other pathways forward to improve mold fidelity could include using ultrasonic energy during the injection of polymer to ensure complete dispersion into the small cavities^[41] or an injection/compression molding procedure similar to hot embossing ^[42].

Polymer Blend Characterization and Testing:

Using these newly formed MN insert molds we were then able to fabricate microneedle patches from a variety of materials. We initially struggled to obtain highly sharp microneedles

from our insert molds, regardless of mold geometry. We suspect that this was due to the comparatively high viscosity of the injected polymer and the comparatively low injection pressure of our pneumatic piston injector system. We experimented with a vast array of polymers, blends, and plasticizers with the hope of finding a suitable mechanically robust polymer which could be injected into the finely detailed cavities of a microneedle mold and extracted without breaking the sharp tips. The blends which showed promise are listed in **Table 1** and a summary of our other findings can be found in the Supplemental **Table S3**, along with rheometry of several polymer blends in **Figure S16**.

Using PCL as a starting point (due to its high flexibility, low melting point and low melt viscosity), we determined that a temperature between 70-90 °C with pre-vaccuum was optimal for the formation of sharp tips in this material (**Figure S17**). However, we also sought to fabricate an injection moldable dissolvable microneedle patch. Polyethylene glycol, (PEG) possessed similar melt characteristics to PCL as well as high solubility in water. We found that pure PEG 100k offered good mechanical strength, while also possessing a low enough melting temperature (65 °C) to avoid damage to sensitive components during injection. However, PEG 100k by itself dissolved rather slowly and we felt it was necessary to augment it with another polymer: in this case a low molecular weight PVP "K15" in order to allow for faster dissolution in the skin. We created two polymer blends which seemed to offer a best-of-both-worlds solution and our efforts resulted in a microneedle base which could be injected at a temperature under 100 °C, along with good mechanical strength^[43], and fast dissolution in moist skin: PEG 100k/PVP 90:10, and PEG 100k/8k/PVP 80:10:10.

Characterization of Microneedles Arrays:

IM microneedles were mechanically tested to investigate their needle breaking strength compared to conventional solvent cast microneedles. The mechanical testing of a PEG 100k/PVP 90:10 polymeric IM MN patch as well as a solvent-cast PVP MN patch is demonstrated in Figure S18 and the results from such testing in Figure S19. It can be seen that while solvent cast microneedles tended to exhibit uniform stress loading, leading to a surprisingly ductile failure of the PVP tips, the PEG/PVP MN patches had uneven strain response, likely due to their uneven needle lengths. The IM patches required nearly 0.4 mm to settle into uniform strain response, and exhibited a similar ductile failure mode to the PVP cast MN patches. This suggests that even though the PEG/PVP IM MN patches have non-uniform tip lengths, their bending load and consequently their ability to penetrate skin may be similar to that of the solvent cast PVP MN patches. The applicability of such tests to real world conditions, however, is limited due to the fact that skin is significantly more compliant and would allow the microneedles to penetrate straight rather than bending over on a non-compliant metal plate.

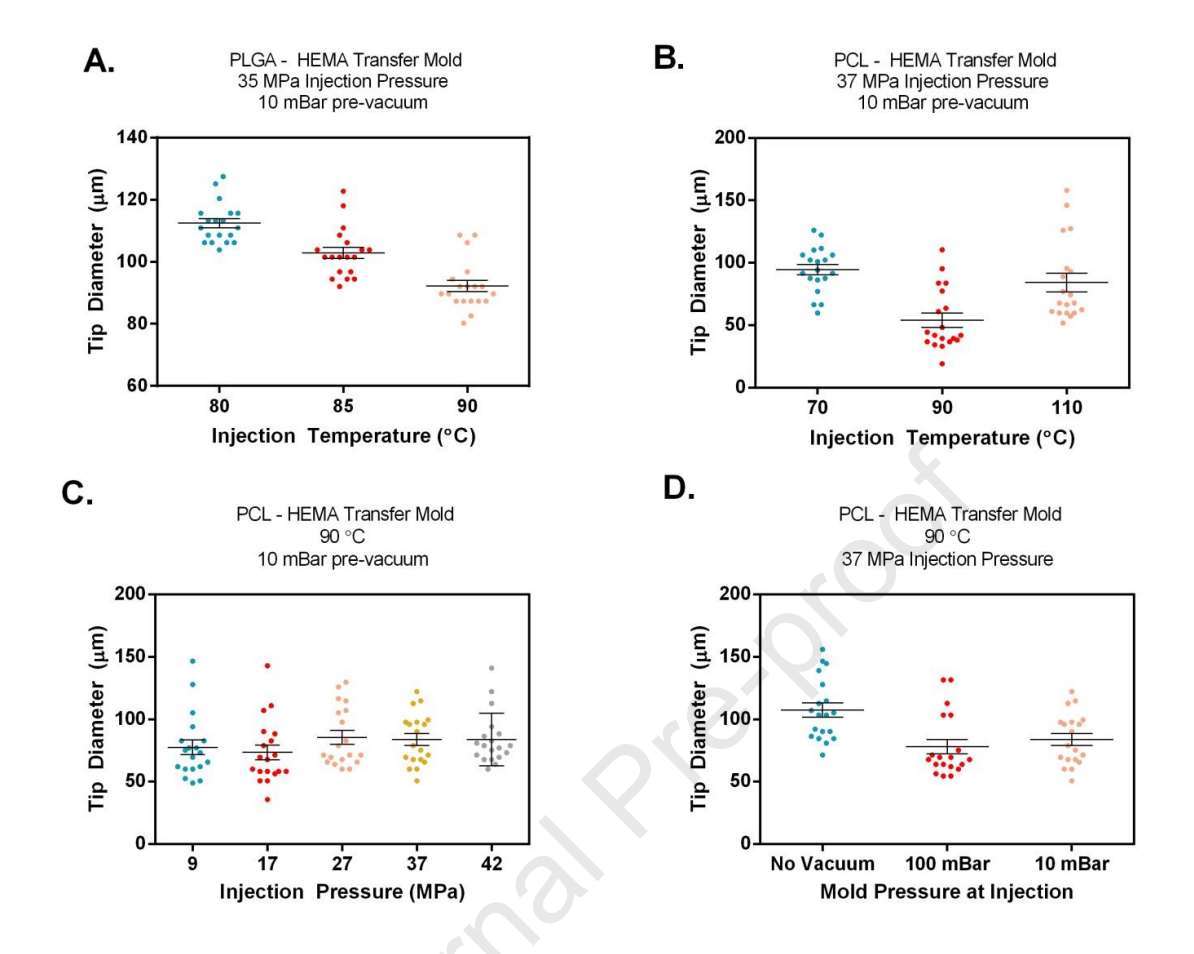


Figure 4: Summary of data taken from electron micrographs of microneedle patches injection molded with a variety of settings showing effect of changes in pressure, temperature, polymer material and use of prevacuum: A) effect of varying injection temperature on PLGA, B) effect of injection temperature on PCL, C) effect of varying injection pressure on PCL, and D) effect of pre-vacuum on tip diameter of PCL. Tip diameter was measured directly by image analysis of MN patch samples via SEM.

For injection molding of PLGA MN patches, we were able to achieve somewhat sharper tips with higher temperatures (**Figure 4A**), but still not as sharp as those molded from PCL. PCL failed to mold at temperatures below 60 °C, but once above its T_m, we found that further increases in temperature had little correlation with tip sharpness (**Figure 4B**). We also found no correlation between tip sharpness and injection pressure for PCL (**Figure 4C**).

The use of pre-vacuum was found to be critical to achieving high sharpness injection molded microneedle arrays. Arrays molded without pre-vacuum were not as sharp as those with

mild or moderate vacuum applied during the injection process (**Figure 4D**, **S17**). We suspect that when injection molding very small features with high aspect ratios, the presence of trapped air plays a large part in determining the sharpness and fidelity of the resultant structures which ordinarily is not seen in macro-scale injection molded parts with comparatively small aspect ratios. This effect is consistent with findings in the literature regarding the improved replication of high aspect-ratio structures using vacuum-assisted venting. The application of even mild vacuum showed a significant improvement in feature resolution over no vacuum. However, the application of a deeper pre-vacuum showed no significant improvement. Furthermore, literature suggests that the application of vacuum reduces the temperature of the flow front in small cavities and thus may prove a hindrance to the injection molding of polymers with higher melting points or higher viscosities. [45]

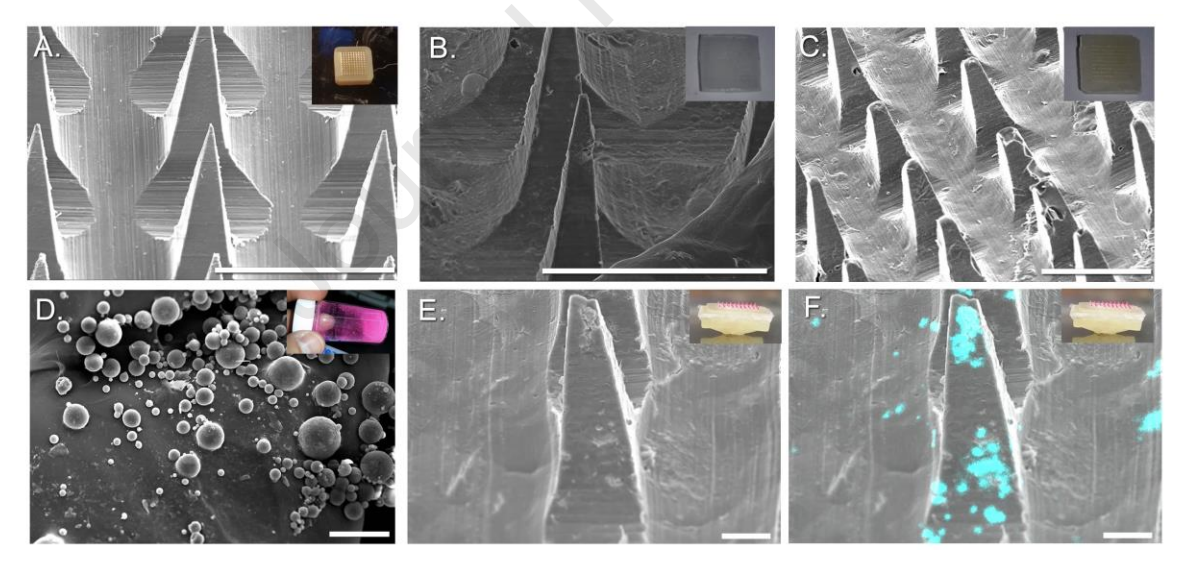


Figure 5: Injection molded microneedles - A) poly 2-Hydroxyethylmethacrylate (pHEMA) positive cast used to form negative microneedle cavity mold, B) injection molded microneedle patch in poly(ε-caprolactam) (PCL), C) injection molded microneedle patch in poly(ethylene glycol) M_w=100,000 (PEG100k), D) PLGA microparticles doped with rhodamine B (for fluorescence microscopy – Pd/C was the dopant for EDS), E) SEM micrograph of PEG100k/poly-Vinyl Pyrrolidone (PVP) dissolvable microneedle patch with PLGA microparticles, and F) EDS Pd L-α composite map showing microparticles concentrated at the tips of needles. Scale bars: A, B, and C: 500 μm, D, E and F: 100 μm.

When injection molding parameters are adjusted correctly, the needles formed from PCL were nearly as sharp as their pHEMA analogues made from commercial solvent-casting molds (Figure 5A, B). However, we found it was more difficult to make sharp microneedles from high molecular weight PEG100k, PLGA, or blends of such. We suspect this was due to their lower mechanical toughness and tendency for small needle tips to break off in the mold rather than pulling out with the base material like those molded in PCL (Figure 5C). Patches fabricated from PLGA presented additional difficulties due to PLGA's high melt viscosity coupled with its comparatively low molecular weight (resulting in poor/brittle mechanical properties), with many patches breaking upon attempts to remove them from the mold.

Microneedles containing embedded microparticles (**Figure 5D**, **and S20**) are especially promising due to the potential to embed active delivery systems or controlled release devices within the microneedle tips allowing for self-administration of prime-boost vaccines to be accomplished in seconds by the end user with controlled drug or vaccine nanoparticle release which could last for weeks or months [46,47]. Microparticles were loaded into the IM insert mold by manually loading dry microparticle powder onto the cavities of the insert mold prior to injection. We found that during injection molding, microparticles consistently remained in the needles as the molten polymer flowed around them. This phenomenon is evident from photography (the red color in the needle tips is due to the presence of RhB-doped PLGA microparticles) and was verified by EDS using Pd/C doped PLGA microparticles (**Figure 5E** and **F**).

Delivery of Microneedle Payload:

To demonstrate needle penetration and in vitro delivery across porcine skin we fabricated fluorescently labeled microneedles embedded with PLGA microparticles containing an orthogonal fluorophore. Dissolvable PEG microneedles with embedded PLGA particles (**Figure 6A**) can be fabricated with high throughput at low temperature (90 °C), and with sharp enough tips to penetrate porcine skin (**Figure 6B, C** shown after 40 N pressure applied for 120 s). Such microneedles not only release their prime payload (shown in green FITC fluorescence in **Figure 6C, D, and E**), but also deposit PLGA microparticles (shown in red RhB fluorescence) up to 440 µm into porcine skin.

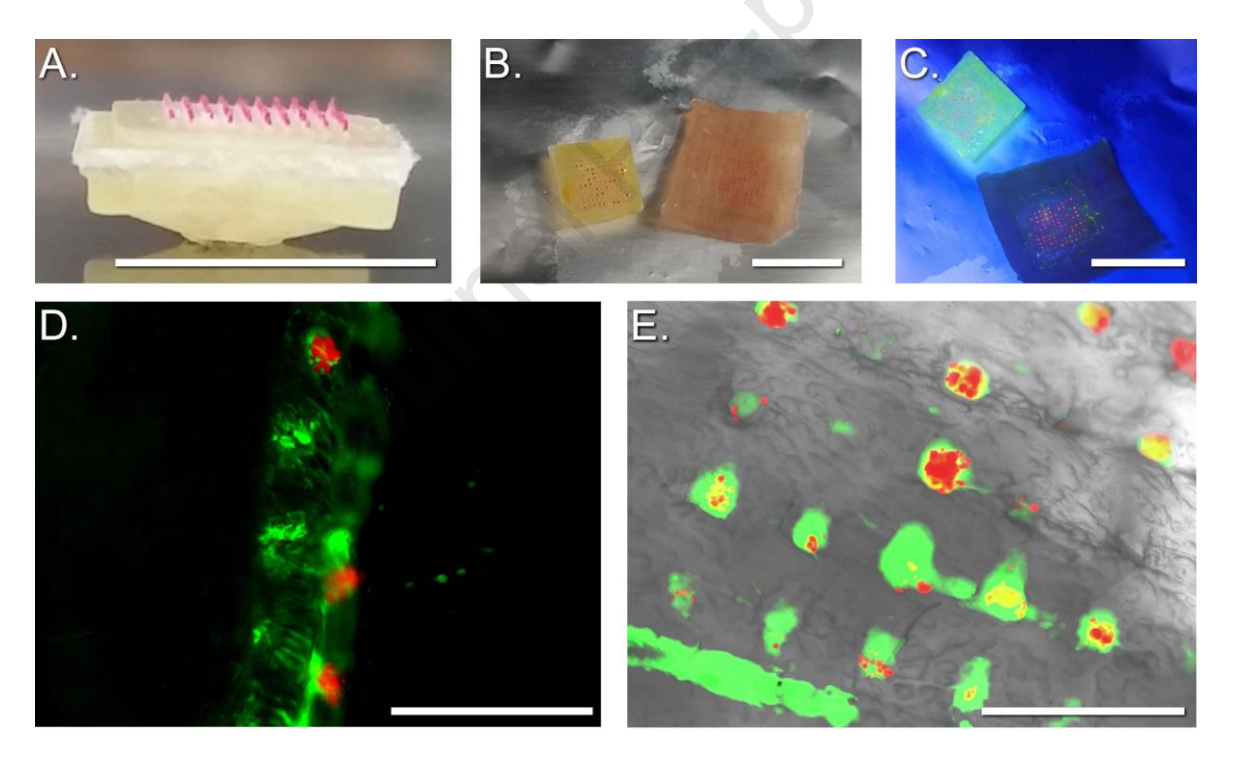


Figure 6: Demonstration of dissolvable microparticle-laden microneedles via an injection molding approach. A) FITC-containing MN patch with Rhodamine-containing MP after de-molding, B) MN patch after pressing into porcine skin using 40N force for 120s under white light, C) under 395 nm UV light, D) composite cross sectional fluorescence micrograph of porcine skin after MN injection, E) composite transmission fluorescence micrograph of porcine skin after MN injection. Scale bars: A-C) 10 mm, D-E) 1 mm.

In the supplementary information, we have attached a GIF video and fluorescence micrographs showing the partial dissolution of a similar patch dissolving in a pH 5.5 20% acrylamide gel. [48] The microneedle patch was pushed into the gel, left to dissolve for 2 minutes, then the patch backing removed and images were taken at 2 minute intervals using a digital fluorescence microscope - showing diffusion of the FITC (green) into the acrylamide gel on the right hand side but the microparticles containing RhB (red) remain in place in their cavities. SEM images of the microparticles (after injection molding with PEG 100k/PVP 90:10, and dissolution of needles in pH 5.5 buffer) show some agglomeration of the PLGA microparticles (Figure S21) which could serve to slow release kinetics but remains to be determined definitively.

Limitations of Microneedle Tip Sharpness:

We found that the sharpness of the microneedle tips (indicating the quality of the injection molded parts by demonstrating a quantitative measure of minimum feature size/aspect ratio) was limited by melt viscosity, mechanical strength of the polymeric material (to retain tips during demolding), and also by an unknown factor which seemed to limit tip diameter to 50-100 µm even in the best-case materials with low melt viscosity (PCL). Exploration of this limitation was pursued, but ultimately left unsolved. We suspect that the thermal mass of the molds may play a pivotal role in this edge case. As the polymer flows and the needle cavity narrows and the polymer's thermal mass decreases in proportion to the reduction in cross sectional area, the temperature of the polymer approaches the temperature of the cold mold, resulting in early solidification prior to full penetration of the needle cavity. This would explain why the epoxy needle molds showed high fidelity at the base of needles, but the tips were blunted. We

attempted tests with molds made from other materials such as stainless steel, which showed poorer fidelity and needle cavity filling (likely due to their increased thermal mass), however our studies on such molds are ongoing. In future iterations we suspect that sharp tips may be obtained by through-drilling the mold insert and applying vacuum through a fritted stainless steel disk to ensure the polymer does not contact the sides of the mold past a certain aspect ratio (roughly 1:8). Pre-heating of the mold insert may also accomplish a similar function, but the current iteration of the prototype is not set up to conduct such tests.

Conclusion:

In the current work we constructed a pilot scale injection molding (IM) machine to demonstrate the production of arbitrary geometries which can be created via pHEMA/epoxy transfer casting or resin 3D printing of interchangeable insert molds on an inexpensive MSLA 3D printer (Anycubic Photon <\$300 MSRP). These epoxy or 3D printed insert molds greatly simplify the system's design and reduce prototyping cost dramatically, allowing greater flexibility in research and development of new geometries and materials for injection molded medical devices. The system has a small bench footprint (1x1 sq ft.) and can be constructed for under \$3,000 which puts it well within the reach of academic and industrial labs who may not have the space or budget for more expensive conventional injection molding systems. Our work includes a full set of plans, CAD drawings, machining documents, bill of materials, STL files, assembly instructions, and injection molding parameters along with an optimization of molding parameters has been provided so that others may replicate and improve upon our system design.

We have also successfully demonstrated a scalable system for the production of dissolvable IM microneedle patches from well-studied polymers (PEG/PLGA/PVP). The sharpness and strength of these microneedles produced has been characterized. Such MN patches could one day hold the key to the delivery of therapeutic doses at scale without the need for low temperature cryopreservation, HCP administration or cold-chain infrastructure. These microneedle patches could be adapted to not only deliver small molecules and therapeutic nanoparticles but to do so with controlled release capability built-in. Samples of microneedles fabricated using our system were characterized via SEM and EDS. Furthermore, porcine skin penetration was conducted to validate the viability and release characteristics of microneedles produced using this method. The production technique we have demonstrated thus far represents a significant step forward in the manufacturing of self-administrable medical devices which may one day aid in the scale and distribution of therapeutics worldwide and help to curb the spread of future pandemics.

Acknowledgments

This work was sponsored in part by the UC San Diego Materials Research Science and Engineering Center (UCSD MRSEC), supported by the National Science Foundation (Grant DMR-2011924), as well as NSF awards OISE 184463 and CMMI 2027668. We would also like to acknowledge the machining expertise and design consulting offered by: Sam Shifron of Ecocell, LLC for his great assistance in machining many of the tight-tolerance metal components used in our apparatus. Ben Whiteside and Pavel Penchev of the University of Birmingham School of Engineering for their machining, laser hole drilling, and optical profilometry of a prototype stainless steel mold insert.

References:

- [1] D. E. Dimla, M. Camilotto, F. Miani, J. Mater. Process. Technol. 2005, 164–165, 1294.
- [2] A. G. Banerjee, X. Li, G. Fowler, S. K. Gupta, Res. Eng. Des. 2007, 17, 207.
- [3] C. D. Ryder, Method of Forming and Injecting Thermoplastic Materials, 1942, US2287277A.
- [4] L. Zema, G. Loreti, A. Melocchi, A. Maroni, A. Gazzaniga, J. Controlled Release 2012, 159, 324.
- [5] Handbook of Molded Part Shrinkage and Warpage, Elsevier, 2013.
- [6] W. Hong-wu, Z. Shao-dan, Q. Jin-ping, X. Hai-hang, Polym.-Plast. Technol. Eng. 2007, 46, 123.
- [7] L. Zema, G. Loreti, A. Melocchi, A. Maroni, A. Gazzaniga, J. Controlled Release 2012, 159, 324.
- [8] J. Giboz, T. Copponnex, P. Mélé, J. Micromechanics Microengineering 2007, 17, R96.
- [9] L. Zema, G. Loreti, E. Macchi, A. Foppoli, A. Maroni, A. Gazzaniga, J. Pharm. Sci. 2013, 102, 489.
- [10] D. M. Wirth, J. K. Pokorski, *Polymer* **2019**, *181*, 121802.
- [11] P. W. Lee, S. Shukla, J. D. Wallat, C. Danda, N. F. Steinmetz, J. Maia, J. K. Pokorski, ACS Nano 2017, 11, 8777.
- [12] P. Lee, J. Towslee, J. Maia, J. Pokorski, Macromol. Biosci. 2015, 15, 1332.
- [13] J. Yu, Y. Zhang, Y. Ye, R. DiSanto, W. Sun, D. Ranson, F. S. Ligler, J. B. Buse, Z. Gu, Proc. Natl. Acad. Sci. 2015, 112, 8260.
- [14] "Zosano Pharma Announces FDA Acceptance of 505(b)(2) New Drug Application for QtryptaTM for the Acute Treatment of Migraine," can be found under https://www.nasdaq.com/press-release/zosano-pharma-announces-fda-acceptance-of-505b2-new-drug-application-for-qtryptatm, n.d.
- [15] "Corium, Inc. Announces FDA Filing Acceptance of New Drug Application for ADLARITY® (donepezil transdermal system) for the Treatment of Alzheimer's Disease," can be found under https://www.biospace.com/article/corium-inc-announces-fda-filing-acceptance-of-new-drug-

- $application-for-adlarity-done pezil-transdermal-system-for-the-treatment-of-alzheimer-s-disease/, \\ \textbf{n.d.}$
- [16] R. Parhi, Intl. J. of Pharm. Sci. and Nano. 2019, 12, 4511.
- [17] N. G. Rouphael, M. Paine, R. Mosley, S. Henry, D. V. McAllister, H. Kalluri, W. Pewin, P. M. Frew, T. Yu, N. J. Thornburg, S. Kabbani, L. Lai, E. V. Vassilieva, I. Skountzou, R. W. Compans, M. J. Mulligan, M. R. Prausnitz, A. Beck, S. Edupuganti, S. Heeke, C. Kelley, W. Nesheim, *The Lancet* 2017, 390, 649.
- [18] J. A. Stinson, C. R. Palmer, D. P. Miller, A. B. Li, K. Lightner, H. Jost, W. C. Weldon, M. S. Oberste, J. A. Kluge, K. M. Kosuda, *Vaccine* 2020, 38, 1652.
- [19] D. M. Bryce, *Plastic Injection Molding: Manufacturing Process Fundamentals Vol. 1, Vol. 1,* Society Of Manufacturing Engineers, Dearborn, **1996**.
- [20] M. Kamal, Injection Molding; Technology and Fundamentals., Hanser Publications, 2009.
- [21] S. Gao, Z. Qiu, J. Ouyang, *Polymers* **2019**, *11*, 151.
- [22] H. Haugen, J. Will, W. Fuchs, E. Wintermantel, J. Biomed. Mater. Res. B Appl. Biomater. 2006, 77B, 65.
- [23] M. E. Gomes, A. S. Ribeiro, P. B. Malafaya, R. L. Reis, A. M. Cunha, *Biomaterials* 2001, 22, 883.
- [24] F. Sammoura, J. Kang, Y.-M. Heo, T. Jung, L. Lin, Microsyst. Technol. 2007, 13, 517.
- [25] Y. Zhang, K. Brown, K. Siebenaler, A. Determan, D. Dohmeier, K. Hansen, *Pharm. Res.* **2012**, *29*, 170.
- [26] R. Hoyle, Eur Med Device Technol 2010, 1.
- [27] J.-S. Deng, M. Meisters, L. Li, J. Setesak, L. Claycomb, Y. Tian, D. Stephens, M. Widman, *PDA J. Pharm. Sci. Technol.* **2002**, *56*, 65.
- [28] M. Heckele, W. K. Schomburg, J. Micromechanics Microengineering 2003, 14, R1.
- [29] L. Eith, R. F. T. Stepto, I. Tomka, Manuf Chem 1987, 58, 21.
- [30] C. König, K. Ruffieux, E. Wintermantel, J. Blaser, J. Biomed. Mater. Res. 1997, 38, 115.

- [31] M. M Crowley, F. Zhang, M. A Repka, S. Thumma, S. B Upadhye, S. K. Battu, J. W McGinity, C. Martin, *Pharmaceutical Applications of Hot-Melt Extrusion: Part I*, 2007.
- [32] M. A Repka, S. Majumdar, S. K. Battu, R. Srirangam, S. B Upadhye, *Application of Hot-Melt Extrusion for Drug Delivery*, **2009**.
- [33] M. D. Shin, S. Shukla, Y. H. Chung, V. Beiss, S. K. Chan, O. A. Ortega-Rivera, D. M. Wirth, A. Chen, M. Sack, J. K. Pokorski, N. F. Steinmetz, *Nat. Nanotechnol.* 2020, 15, 646.
- [34] World Health Organization, "WHO | Immunization supply chain and logistics IVB/14.05," can be found under https://apps.who.int/iris/bitstream/handle/10665/131568/WHO_IVB_14.05_eng.pdf, n.d.
- [35] United Nations, Population Division, "WHO | Global Vaccine Action Plan 2019 Immunization coverage data," can be found under

 https://www.who.int/immunization/monitoring_surveillance/who-immuniz.pdf, n.d.
- [36] H. Juster, B. van der Aar, H. de Brouwer, *Polym. Eng. Sci.* **2019**, *59*, 877.
- [37] B. Bediz, E. Korkmaz, R. Khilwani, C. Donahue, G. Erdos, L. D. Falo, O. B. Ozdoganlar, *Pharm. Res.* **2014**, *31*, 117.
- [38] N. R. Nair, V. C. Sekhar, K. M. Nampoothiri, A. Pandey, in Curr. Dev. Biotechnol. Bioeng. (Eds.: A. Pandey, S. Negi, C. R. Soccol), Elsevier, 2017, pp. 739–755.
- [39] "Poly(ethylene oxide) 181986," can be found under https://www.sigmaaldrich.com/catalog/product/aldrich/181986, **n.d.**
- [40] N. Passerini, D. Q. Craig, J. Control. Release Off. J. Control. Release Soc. 2001, 73, 111.
- [41] D. E. Ferguson, S. K. Nayar, D. L. Pochardt, Method of Molding a Microneedle, 2012, US8246893B2.
- [42] K. Nagato, *Polymers* **2014**, *6*, 604.
- [43] A.-Y. Jee, H. Lee, Y. Lee, M. Lee, Chem. Phys. 2013, 422, 246.
- [44] S. Ying Choi, N. Zhang, J. P. Toner, G. Dunne, M. D. Gilchrist, J. Micro Nano-Manuf. 2016, 4, DOI 10.1115/1.4032891.

- [45] M. Sorgato, M. Babenko, G. Lucchetta, B. Whiteside, Int. J. Adv. Manuf. Technol. 2017, 88, 547.
- [46] M. A. Lopez-Ramirez, F. Soto, C. Wang, R. Rueda, S. Shukla, C. Silva-Lopez, D. Kupor, D. A. McBride, J. K. Pokorski, A. Nourhani, N. F. Steinmetz, N. J. Shah, J. Wang, *Adv. Mater.* 2020, 32, 1905740.
- [47] C. E. Boone, C. Wang, M. A. Lopez-Ramirez, V. Beiss, S. Shukla, P. L. Chariou, D. Kupor, R. Rueda, J. Wang, N. F. Steinmetz, ACS Appl. Nano Mater. 2020, 3, 8037.
- [48] S. F. Lahiji, M. Dangol, H. Jung, Sci. Rep. 2015, 5, DOI 10.1038/srep07914.

- Assembly of a gram-scale injection molding system with 3D printed inserts
- Melt processing of polymers at high temperature and pressure
- Demonstration of dissolvable solvent-free injection molded microneedle patches
- Method for the fabrication of microneedle injection molds
- Facile production of 3D printed mold inserts for rapid swap and production of arbitrary shapes

Declaration of Competing Interest

Dr. Pokorski is a co-founders of, has equity in, and has a financial interest with Mosaic ImmunoEngineering Inc. Dr. Pokorski serves as scientific advisor and paid consultant to Mosaic. The other authors declare no potential conflicts of interest.

Credit Author Statement

David Wirth: Conceptualization, methodology, validation, formal analysis, writing – original draft, review, editing. **Leonard McCline**: methodology, investigation, writing-editing. **Jonathan Pokorski**: Conceptualization, resources, writing-editing, supervision, project administration, funding acquisition.